Cylindrical and Row Trenched Cooling Holes with Alignment Angle of 90° at Different Blowing Ratios

Ehsan Kianpour, Nor Azwadi Che Sidik[*] and Mazlan Abdul wahid

Faculty of Mechanical Engineering, Universiti Teknologi Malaysia
81310 UTM Johor Bahru, MALAYSIA

Abstract

This study was carried out to find out the effects of two different blowing ratios of BR=1.25 and BR=3.18 on the film cooling performance adjacent the combustor end wall, whereas two different cooling holes arrangements as cylindrical and row trenched cooling holes with alignment angle of 90 degree are considered. In this research, a three-dimensional presentation of a true Pratt and Whitney aero-engine was simulated and analyzed with a commercial finite volume package FLUENT 6.2.26 to gain fundamental data. The current study has been performed with Reynolds-averaged Navier-Stokes turbulence model (RANS) on internal cooling passages. This combustor simulator combined the interaction of two rows of dilution jets, which were staggered in the stream wise direction and aligned in the span wise direction. The entire findings of the study declared that with using the row trenched holes near the enwall surface; film cooling effectiveness is doubled compared to the cooling performance of baseline case.

Keywords: Gas Turbine; Film-Cooling; Cylindrical Hole; Trenched hole; Blowing Ratio.

1. Introduction

Gas turbine industries try for higher engine efficiencies. Bryton cycle is a key to this study. According to this cycle, the turbine inlet temperature should increase to gain more efficiency. However increasing the turbine inlet temperature creates an extremely harsh environment for critical downstream components such as turbine vanes. So, it is needed to design a cooling technique in this area. Film cooling is the traditional way which is used. In this system, a thin thermal boundary layer such as buffer zone is formed and attached on the protected surface. Cylindrical and trenched cooling holes are two layouts of these holes. With trenching the cooling holes, the injected coolant is suddenly spread before exiting the cooling holes and entering the main flow and as a result the coolant attached better on the surface. According to the importance of this research, a broad literature search was conducted to collect the information. Stitzel and Thole [1] indicated that dilution jet injection is the dominant feature at the combustor exit, while with no dilution, the exit profile was relatively uniform with a high temperature and low total pressure flow in the mainstream. Furthermore, Scrittore [2] mentioned that increasing the dilution jet velocity adversely effects the surface cooling performance downstream of dilution jets. Vakil and Thole [3]

and Barringer et al. [4] presented experimental results of the combustor simulator. In this study, a real large scale of combustor was simulated and the coolant flow and high momentum dilution jets were spread into the main flow. The results showed that high temperature gradient was developed upstream of the dilution holes. The injection of the flow from the first row of dilution holes lead to the combustor temperature decrease by 25%. The results indicated that while, the dilution jets declined the total pressure and velocity fields, the turbulence level at the end of combustor reached to 24%. This quantity is under predicted compared to Colban et al. [5] findings which defined the turbulence level between 25 to 30 percent. Kianpour, Azwadi and Mirzabozorg [6,7] simulated the combustor endwall cooling holes with two different layouts and exit section area. The results declared that while, the central part of the jets stayed nominally at the same temperature level for both configurations, the temperatures adjacent the wall and between the jets was a while cooler with less cooling holes.

In order to specify the net heat flux reduction, Harrison et al. [8] studied the effects of film cooling and heat transfer coefficient around the trenched axial hole over the suction surface of turbine vane. The results showed that at low blowing ratios both cylindrical and trenched holes had similar behavior, however, increasing blowing ratio led to cooling performance dramatic reduction for cylindrical holes and cooling effectiveness enhancement for trenched holes and it is concurred with Shupping [9] and Baheri Islami and Jurban [10] findings. Yiping et al. [11] tested the effects of depth and width of trenches on the film cooling under overall cooling effectiveness of ϕ=0.6 as determined by Maikell et al. [12]. This constant value of overall cooling effectiveness declared that at the leading edge, the thermal barrier coating has moderate dependency to the stagnation line variation. Also it is figured out that the third (w=2.0D and d=0.75D) and fourth (w=3.0D and d=0.75D) case were more effective than other cases and base line case and it means the trench depth of 0.75D was the optimum one as well as approved by CFD studies. Sundaram and Thole [13] and Lawson and Thole [14] studied the effects of trenched depth and width on film cooling performance at the vane-end Wall. The results showed that the maximum cooling effectiveness is obtained at the trench depth of 0.80D. However, Lawson and Thole stated that the trench depth of 0.8D has negative effect on the cooling performance downstream the cooling hole.

However, till now, investigation into the effects of trenching the cooling holes near the combustor end wall surface on the film cooling effectiveness have not been carried out. There are several unanswered questions: How do cylindrical and trenched cooling holes perform at different blowing ratios? Therefore the objective of the present study was to investigate the film cooling effectiveness variation with different arrangements of cooling holes and blowing ratios. Also in order to measure the validity of the results, a comparison between the data gained from this study and Vakil and Thole [3] project was done.

2. Methods and Materials

In this study a three-dimensional representation of a true Pratt and Whitney engine was simulated and analyzed to gain essential data. The schematic view of the combustor is shown in Figure 1. The final combustor simulator design width and inlet height was 111.8 cm and 99.1 cm respectively. The length of the combustor was 156.9 cm and the contraction angle was 15.8 degree. The contraction angle began at X=79.8 cm. The inlet cross sectional area was 1.11 square meters and the exit cross sectional area was reduced to 0.62 square meters. The combustor simulator included four film-cooled stream wise panels. The starting point of these panels was approximately at 1.6m upstream of the turbine vanes. The first and second panels were 39.2 and 40.6 cm in length. The length of the next two panels was 36.8 cm and 43.2 cm. The low thermal conductivity of combustor panels were 1.27 cm in thickness allowed for adiabatic surface temperature measurements. Two different rows of dilution holes were considered within the second and third panels. These dilution rows were located at 0.67 m and 0.90 m downstream of the beginning of the

combustor liner panels. The diameter of the first row and second row of dilution holes was 8.5 cm and 11.9 cm respectively.
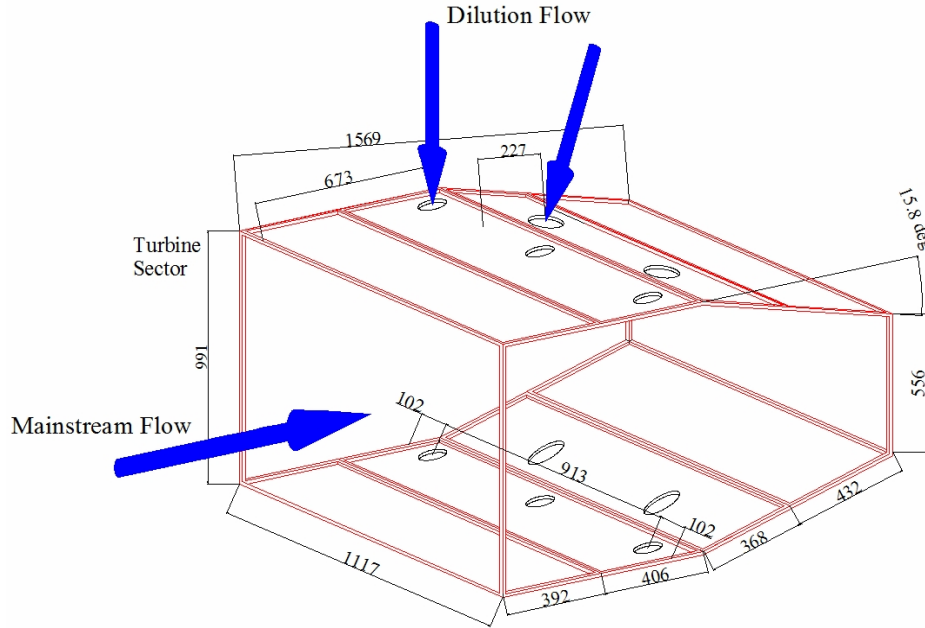
Figure 1. The 3-D view of the combustor simulator

The centreline of the second row was staggered with respect to the first row of dilution holes. To verify the purpose of this study, a three-dimensional representation of a Pratt and Whitney gas turbine engine was simulated. The present combustor simulator included two configurations of cooling holes. The first arrangement (baseline) was designed similar to the Vakil and Thole [3]. In both cases, the film cooling holes were placed in equilateral triangles. The diameter of the film cooling holes was 0.76 cm and drilled at an angle of 30 degree from the horizontal surface. The length of film cooling holes in the baseline case was 2.5 cm. For the second case (case 2) the cooling holes embedded within a row trench with alignment angle of 90 degree which is shown in Figure 2. Furthermore, the trench depth and width was 0.75D and 1.0D respectively. A global coordinate system (X, Y and Z) was also selected.
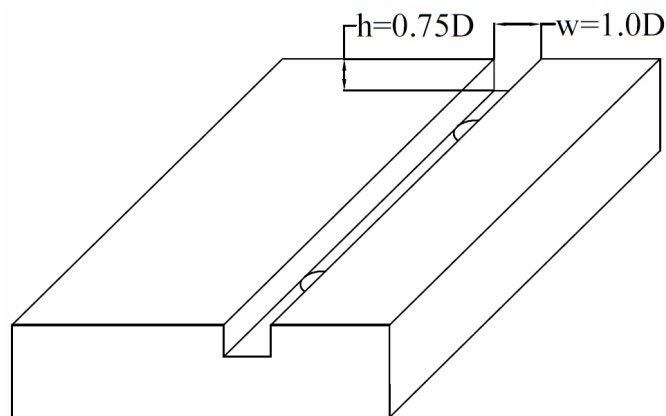
Figure 2. The schematic of row trenched cooling holes with alignment angle of 0 degree

The thermal distribution inside a combustor simulator was measured along the specific measurement planes. These measurement planes are shown in Figure3.In order to get more accurate

data and reasonable time consumption, about 8×106 tetrahedral meshes were used and this is in concurred with Stitzel and Thole [1] study.
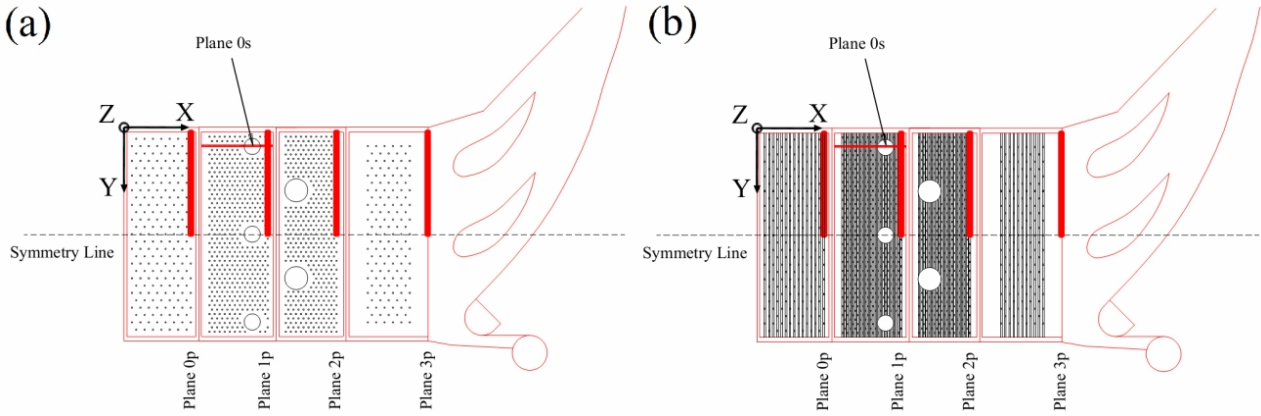

Figure 3. Location of the measurement planes (a) baseline (b) Case 2

According to the specific flow ratio at the inlet of volume control, inlet mass flow boundary condition was defined. Wall boundary condition and slip less boundary condition were applied to limit the interaction zone between fluid and solid layer. Also at the end of volume control the pressure outlet boundary condition was used. In addition, both cases were completely symmetric along the X-Y and X-Z planes. According to this issue, symmetry boundary condition $\partial\partial n=0$ was applied. In addition theses equations were used as well.

Continuity equation:

$$\frac{\partial \rho}{\partial t} + \frac{\partial}{\partial x}\frac{dx}{dt} + \frac{\partial \rho}{\partial y}\frac{dy}{dt} + \frac{\partial \rho}{\partial z}\frac{dz}{dt} = -\rho(\nabla . V) \tag{1}$$

Momentum equation:

$$\frac{\partial}{\partial t}(\rho u_i) + \frac{\partial}{\partial x_j} = (\rho u_i u_j) = -\frac{\partial P}{\partial x_i} + \frac{\partial \tau_{ij}}{\partial x_i} + \rho g_i + \vec{F_i} \tag{2}$$

Energy equation:

$$\frac{\partial}{\partial t}(\rho E) + \frac{\partial}{\partial x_i}\left(u_i(\rho E + P)\right) = \frac{\partial}{\partial x_i}\left(K_{eff}\frac{\partial T}{\partial x_i} - \sum_j h_j J_j + u_j(\tau_{ij})_{erf}\right) + S_h \tag{3}$$

and RNG K-ε equation:

$$\frac{\partial}{\partial t}(\rho k) + \frac{\partial}{\partial x_i}(\rho k u_i) = \frac{\partial}{\partial x_j}\left[\left(\mu + \frac{\mu_t}{\sigma_k}\right)\frac{\partial k}{\partial x_j}\right] + P_k - \rho\epsilon \tag{4}$$

$$\frac{\partial}{\partial t}(\rho \epsilon) + \frac{\partial}{\partial x_i}(\rho \epsilon u_i) = \frac{\partial}{\partial x_j}\left[\left(\mu + \frac{\mu_t}{\sigma_\epsilon}\right)\frac{\partial \epsilon}{\partial x_j}\right] + C_{1\epsilon}\frac{\epsilon}{k}P_k - C_{2\epsilon}^*\rho\frac{\epsilon^2}{k} \tag{5}$$

To understand the thermal field results, the quantities should be defined. Film cooling effectiveness is defined as below:

$$\eta = \frac{T - T_\infty}{T_C - T_\infty} \tag{6}$$

In the above equation T is the local temperature, T_∞ is main stream temperature and T_C is the temperature of coolant.

3. Findings and Discussion

The comparison has been made for baseline case among the numerical results by Stitzel and Thole [1], experimental results by Vakil and Thole [3], and the current study. Figure 4 presents the comparison of film cooling effectiveness for plane 1p and 2p at Y/W=0.4. The deviations between the current computation and benchmarks were calculated as follows:

$$\%\text{Diff} = \frac{\sum_{i=1}^n \frac{x_i - x_{i,benchmark}}{x_{i,benchmark}}}{n} \times 1 \tag{7}$$

According to this formula, the deviation was equal to 9.76% and 8.34% compared to Ref [3] and Ref [1] for plane 1p and equal to 13.36% and 11.96% compared to Ref [3] and Ref [1] for plane 2p.
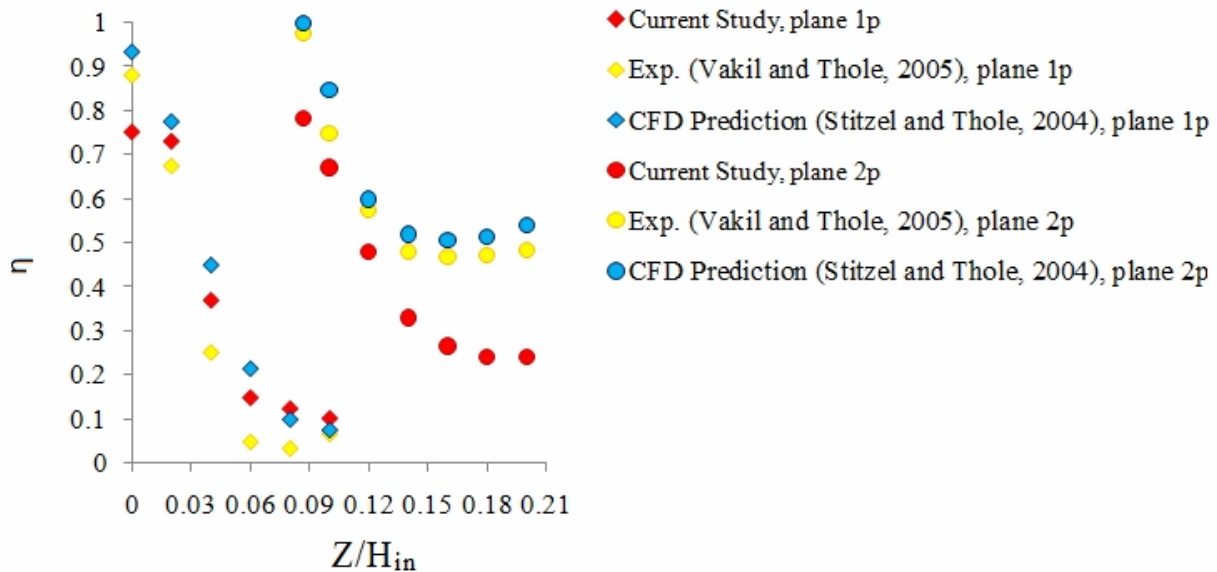

Figure 4. The comparison of film cooling effectiveness for plane 1p and 2p along Y/W=0.4

The film cooling distribution of plane 0p under two different blowing ratios (M=1.25 and M=3.18) is illustrated in figure 5. A significant difference between these figures is the layer of film cooling thickness. While, for the trenched condition, the thickness of this layer reached to Z=50mm at blowing ratio of 1.25, under the blowing ratio of M=3.18, it reached to Z=90mm. However, for this measurement plane, the thicker film cooling layer for the trenched hole does not automatically suggest that is desirable. Of course, for the trenched case and at a position of 31cm<Y<36cm, the temperature level is higher near the endwall surface at M=3.18 compared to the temperature distribution contour of case 2 and at blowing ratio of M=1.25.

The film cooling effectiveness distribution of plane 1p at two different blowing ratios of M=1.25 and M=3.18 is illustrated in figure 6. The film cooling effectiveness was significantly increased between both ratios. At the right side (50cm<Y<54cm) of thermal field contours and for both blowing ratios, film cooling is being entrained by upward motion of dilution jet. Also, at the position of 18cm<Y<40cm and 8cm<Z<10cm is slightly hotter (0<η<0.05) for the trenched case at M=3.18 as opposed to the baseline. However, for both mass flux ratios and adjacent the endwall surface, row trenched hole performs better compared to baseline. The v and w velocity vectors of plane 1p are shown as well. Due to the effect of dilution injection on the thermal behavior of flow,at the middle of the temperature distribution contour, a significant movement of vortexes toward the left and right sides is seen.

Figure 7 shows the distribution of film cooling effectiveness for plane 2p under blowing ratios of M=1.25 and M=3.18. It is highlighted from the contours that the rotating flow is seen on the left side and this is entrained along the span wise direction. However, with mass flux ratio increase, this rotating flow is become weaker; especially for the trenched case. Overwhelmingly apparent, however is the lack of uniformity within the combustor exiting profile at this point. Also, at the right side of film cooling effectiveness distribution for baseline, it is found that hot gases covered more extended area in comparison with trenched cases. Note that, the film cooling effectiveness reduction happened due to the blowing ratio enhancement for the baseline. Lastly, these figures show the v and w velocity vectors superimposed on the thermal field contours of this measurement plane. The sweeping of the coolant toward the second row of dilution jet is visible for all cases.
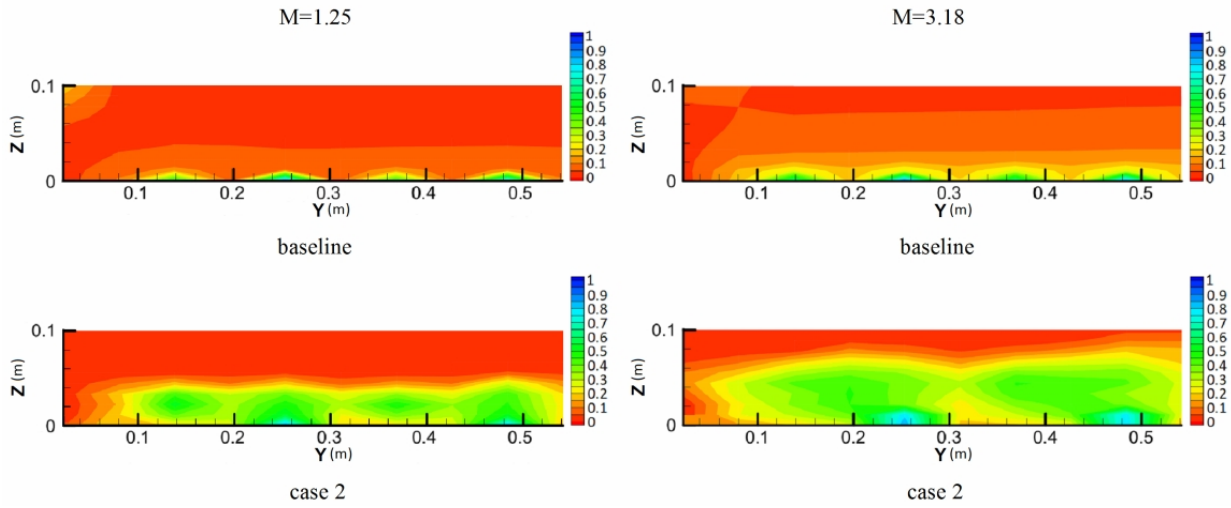
Figure 5. Film cooling effectiveness distribution of plane 0p for different configurations and blowing ratios M=1.25 and M=3.18
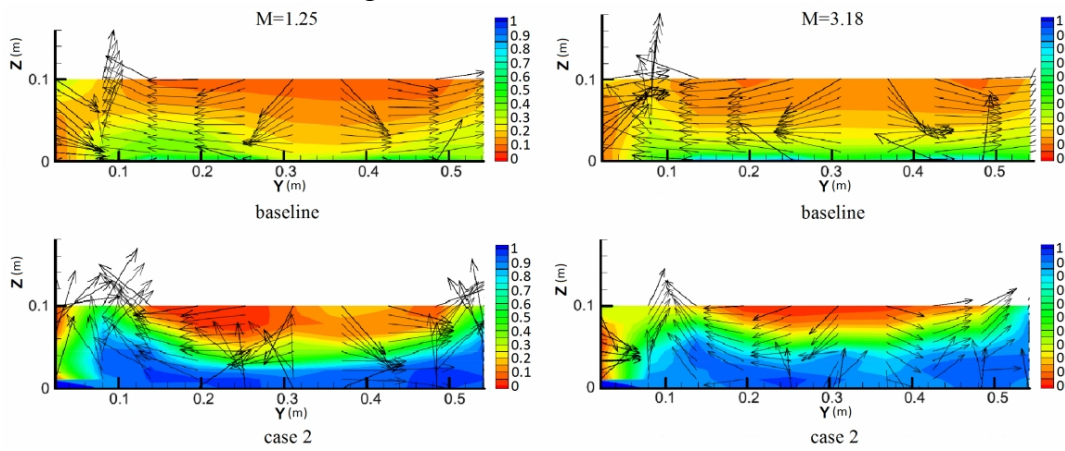
Figure 6. The vectors of v and w with film cooling effectiveness contours of plane 1p for different configurations and blowing ratios BR=1.25 and BR=3.18
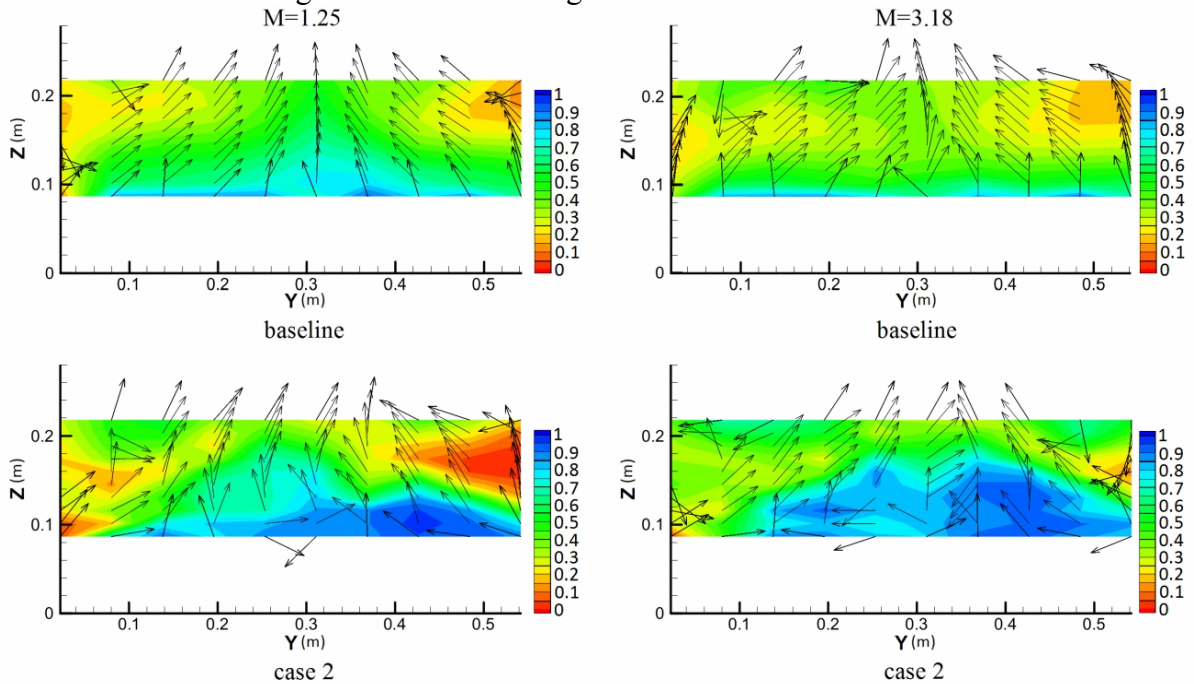
Figure 7. The vectors of v and w with film cooling effectiveness contours of plane 2p for different configurations and blowing ratios BR=1.25 and BR=3.18

The variations of film cooling effectiveness for different measurement planes and mass flux ratios at Y=30cm and along Z axis are shown in figure 8. It is debated that while, for the measurement plane 0p and 1p and for all configurations, the film cooling effectiveness increase occurred with blowing ratio enhancement, for the plane 2p, the film cooling performance reduced about 12% with blowing ratio increase for the baseline. Lastly for plane 3p, the film cooling effectiveness of baseline, increased intensively (58%) so that it is more than trenched cases at high blowing ratio. Also, it is found that case 2 has sever effect on film cooling performance enhancement with blowing ratio increase, especially for measurement plane of 0p and 1p with enhancement ratio of 180% and 203% respectively.

Figure 9 shows the streamwise film cooling distribution through a first row of dilution jet for all configurations at M=1.25 and M=3.18. Note, at the position of 60cm<X<72cm, the dilution jet injected into the mainstream and the coolest region is created. Furthermore, upstream the dilution jet, the hot region Figures is approximately disappeared for the trenched cases and it is happened due to the effects of coolant penetration from trenched cooling holes.
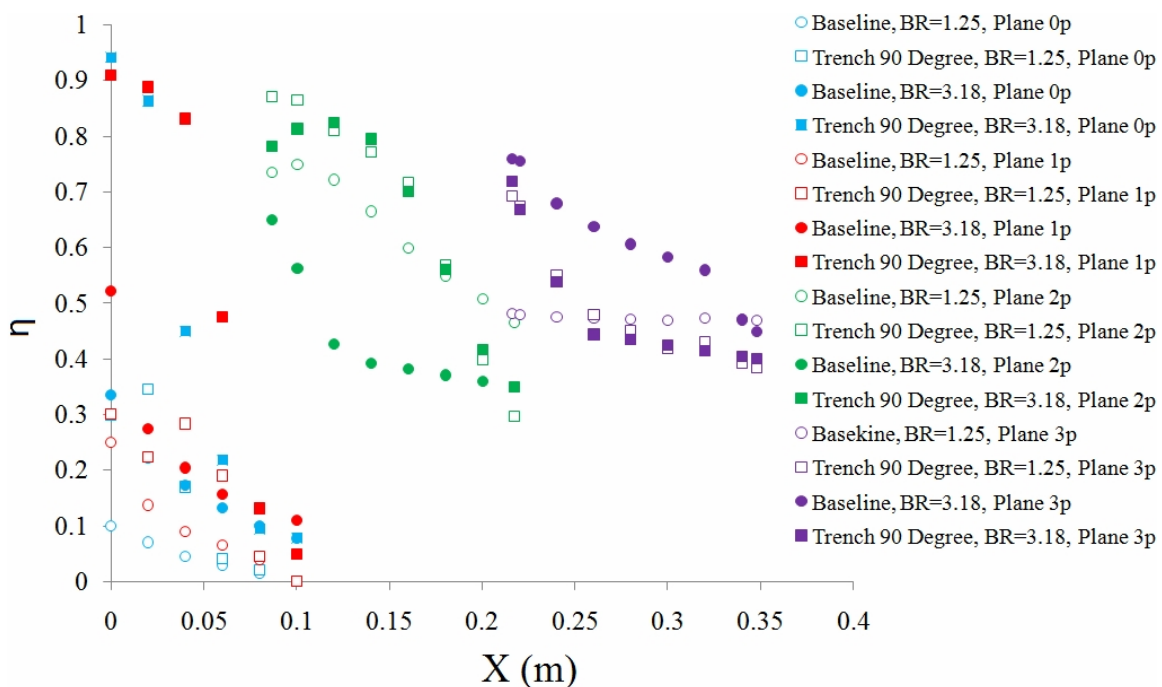

Figure 9. The changes of film cooling effectiveness for different configurations

4. Conclusion and Recommendation

The objective of this study was to analyze the effects of different blowing ratios of M=1.25 and M=3.18 on the film cooling effectiveness with different cooling holes configurations of cylindrical and row trenched holes with alignment angle of 90 degree at the end of combustor simulator. In this study a three-dimensional representation of a Pratt and Whitney engine was simulated and analyzed. To sum up, while, for all layouts, the film cooling layer is growing at high mass flux ratio, it becomes thinner by using cylindrical holes for plane 2p. Also, the central part of the plane 2p showed the intense penetration of the coolant and a thick film cooling layer creation in the trenched cases. On the other hand, blowing ratio increase led to have a cooler region adjacent the wall and between the jets, especially for the trenched cases. The thermal field findings demonstrated a recirculation area developed exactly downstream of the jet where the entrainment of film cooling was caused by the dilution jet. The contours of the stream wise thermal field indicate the intense effect of trenched cooling holes and dilution injection downstream the dilution jet, particularly for the trenched holes and elevated mass flux ratio. For the measurement plane 0p and

1p and for all configurations, the film cooling effectiveness increase occurred with blowing ratio enhancement, for the plane 2p, the film cooling performance reduced with blowing ratio increase for the baseline. Based on the results and conclusions of the study, there are several recommendations to consider. In future research within this area, it is strongly recommended to use the trenched holes for the second and third cooling panels because, the trenching cooling holes has better effect on film cooling performance at higher blowing ratio.
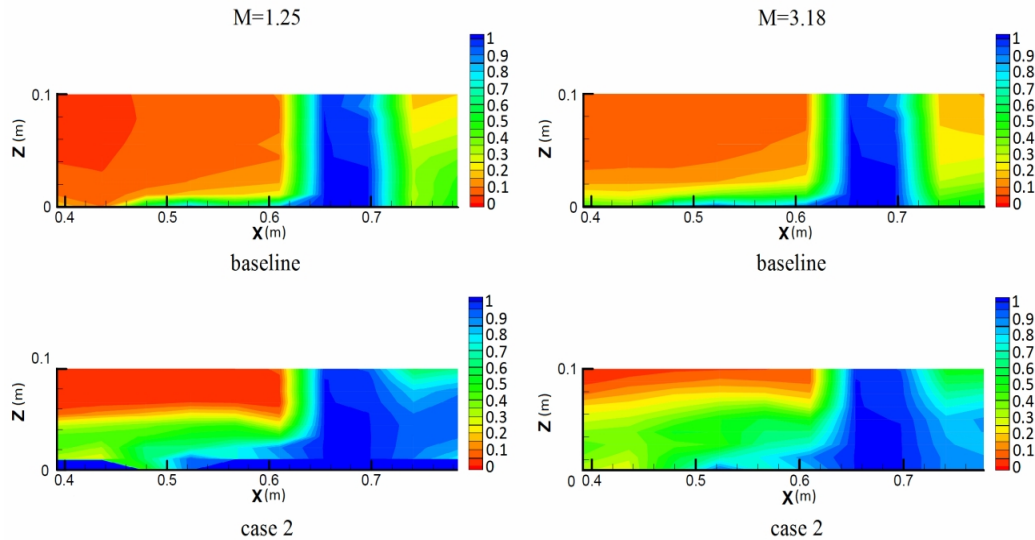

Figure 10. Film cooling effectiveness distribution of plane 0s for different configurations and blowing ratios BR=1.25 and BR=3.18.

References

[1]   Stitzel, S., and K.A. Thole, *Flow Field Computations of Combustor-Turbine Interactions Relevant to a Gas Turbine Engine*. Journal of Turbomachinery, 2004. 126(1): p. 122-129.

[2]   Scrittore, J.J. Experimental Study of the Effect of Dilution Jets on Film Cooling Flow in a Gas Turbine Combustor. PhD theses. Virginia Polytechnic Institute and State University, Virginia. 2008 pp 160

[3]   Vakil, S.S., and K.A. Thole, *Flow and Thermal Field Measurements in a CombustorSimulator Relevant to a Gas Turbine Aero engine*. Journal of Engineering for Gas Turbines and Power, 2005. 127(2): p. 257-267.

[4]   Barringer, M.D., O.T. Richard, J.P. Walter, S.M. Stitzel, and K.A. Thole, *Flow Field Simulations of a Gas Turbine Combustor*. Journal of Turbomachinery, 2002. 124(3): p. 508-516.

[5]   Colban, W.F., A.T. Lethander, K.A. Thole, and G. Zess, *Combustor TurbineInterface Studies—Part 2: Flow and Thermal Field Measurements*. Journal of Turbomachinery, 2003. 125(2): p. 203-209.

[6]   Kianpour, E., C. S. N. Azwadi, and M. Agha Seyyed Mirza Bozorg, *ThermodynamicAnalysis of Flow Field at the End of Combustor Simulator. AEROTECH IV Conference 2012 AMM.225.261*. 2012. KualaLumpur, Malaysia.

[7]   Kianpour, E., C. S. N. Azwadi, and M. Agha Seyyed Mirza Bozorg, *Dynamic Analysis of Flow Field at the Endof Combustor Simulator*. Jurnal Teknologi, 2012. 58(2): p. 5–12.

[8]   Harrison, K.L., J.R. Dorrington, J.E. Dees, D.G. Bogard, and R.S. Bunker, *Turbine Airfoil Net Heat Flux Reduction With Cylindrical Holes Embedded in a TransverseTrench*. Journal of Turbomachinery, 2009. 131(1): p. 011012-1-011012-8.

[9]   C.Shuping, Film Cooling Enhancement With Surface Restructure, PhD theses,University of Pittsburgh, Pennsylvania, pp. 150, 2008.

[10]   Islami, S.B., and B.A. Jubran, *The effect of turbulence intensity on film cooling of gas turbine blade from trenched shaped holes*. Journal of Heat and Mass Transfer, 2012. 48(5): p. 831-840.

[11]   Yiping, L., A. Dhungel, S.V. Ekkad, and R.S. Bunker, *Effect of Trench Width and Depth on Film Cooling From Cylindrical Holes Embedded in Trenches*. Journal of Turbomachinery, 2008. 131(1): p. 011003-1-011003-13.

[12]   Maikell, J., D. Bogard, J. Piggush, and A. Kohli, *Experimental Simulation of a Film Cooled Turbine Blade Leading Edge Including Thermal Barrier Coating Effects*. Journal of Turbomachinery, 2010. 133(1): p. 011014-1-011014-7.

[13]   Sundaram, N., and K.A.Thole, *Bump and Trench Modifications to Film-Cooling Holes at the Vane-End wall Junction*. Journal of Turbomachinery, 2008. 130(4): p. 041013-1-041013-9.

[14]   Lawson, S.A., and K.A.Thole, *Simulations of Multiphase Particle Deposition on End wall Film-CoolingHoles in Transverse Trenches*. Journal of Turbomachinery, 2012. 134(5): p. 051040-1-051040-10.